British Journal of Pharmacology

DOI:10.1111/j.1476-5381.2011.01215.x
www.brjpharmacol.org

RESEARCH PAPER

Effects of rosiglitazone on the configuration of action potentials and ion currents in canine ventricular cells

N Szentandrássy[1], G Harmati[1], L Bárándi[1], J Simkó[2], B Horváth[1], J Magyar[1], T Bányász[1], I Lőrincz[3], A Szebeni[4], V Kecskeméti[4] and PP Nánási[1]

[1]*Department of Physiology, University of Debrecen, Debrecen, Hungary,* [2]*Department of Cardiology, Institute of Medicine, Semmelweis Health Care Center, Miskolc, Hungary,* [3]*Department of Internal Medicine, University of Debrecen, Debrecen, Hungary, and* [4]*Department of Pharmacology and Pharmacotherapy, Semmelweis University, Budapest, Hungary*

Correspondence
Péter P. Nánási, Department of Physiology, University of Debrecen, H-4012 Debrecen, P.O.Box 22, Hungary. E-mail: nanasi@phys.dote.hu

Keywords
antidiabetic agents; rosiglitazone; dog cardiomyocytes; action potential; ion currents

Received
25 September 2010
Revised
21 October 2010
Accepted
28 October 2010

BACKGROUND AND PURPOSE

In spite of its widespread clinical application, there is little information on the cellular cardiac effects of the antidiabetic drug rosiglitazone in larger experimental animals. In the present study therefore concentration-dependent effects of rosiglitazone on action potential morphology and the underlying ion currents were studied in dog hearts.

EXPERIMENTAL APPROACH

Standard microelectrode techniques, conventional whole cell patch clamp and action potential voltage clamp techniques were applied in enzymatically dispersed ventricular cells from dog hearts.

KEY RESULTS

At concentrations ≥10 μM rosiglitazone decreased the amplitude of phase-1 repolarization, reduced the maximum velocity of depolarization and caused depression of the plateau potential. These effects developed rapidly and were readily reversible upon washout. Rosiglitazone suppressed several transmembrane ion currents, concentration-dependently, under conventional voltage clamp conditions and altered their kinetic properties. The EC_{50} value for this inhibition was 25.2 ± 2.7 μM for the transient outward K^+ current (I_{to}), 72.3 ± 9.3 μM for the rapid delayed rectifier K^+ current (I_{Kr}) and 82.5 ± 9.4 μM for the L-type Ca^{2+} current (I_{Ca}) with Hill coefficients close to unity. The inward rectifier K^+ current (I_{K1}) was not affected by rosiglitazone up to concentrations of 100 μM. Suppression of I_{to}, I_{Kr}, and I_{Ca} was confirmed also under action potential voltage clamp conditions.

CONCLUSIONS AND IMPLICATIONS

Alterations in the densities and kinetic properties of ion currents may carry serious pro-arrhythmic risk in case of overdose with rosiglitazone, especially in patients having multiple cardiovascular risk factors, like elderly diabetic patients.

LINKED ARTICLE

This article is commented on by Hancox, pp. 496–498 of this issue. To view this commentary visit http://dx.doi.org/10.1111/j.1476-5381.2011.01281.x

Abbreviations

APD_{50}, action potential duration measured at 50% level of repolarization; APD_{90}, action potential duration measured at 90% level of repolarization; I_{Ca}, L-type Ca^{2+} current; I_{K1}, inward rectifier K^+ current; I_{Kr}, rapid delayed rectifier K^+ current; I_{Na}, Na^+ current; I_{to}, transient outward K^+ current; V_{max}, maximum velocity of depolarization

Introduction

Rosiglitazone is a thiazolidinedione oral hypoglycemic agent active in both diabetic animal models and patients with type 2 diabetes (Quinn *et al.*, 2008; Doshi *et al.*, 2010). Rosiglitazone, similarly to other thiazolidinediones, like troglitazone or pioglitazone, is a high affinity ligand for the peroxisome proliferator-activated receptor-γ, which is responsible for the

insulin-sensitizing action of the compound (Berger *et al.*, 1996; Welters *et al.*, 2004). Beyond improving glycemic control, rosiglitazone and pioglitazone have been shown to exert some cardiovascular benefits (Khandoudi *et al.*, 2002; Cuzzocrea *et al.*, 2003). In contrast, several large clinical studies reported that thiazolidinedione therapy was associated with cardiovascular complications (Krentz, 2009; Kaul *et al.*, 2010). Increased risk of congestive heart failure was observed with the use of both pioglitazone and rosiglitazone (Gerstein *et al.*, 2006; McGuire and Inzucchi, 2008; DREAM Trial Investigators, 2008), while the increased risk of acute myocardial infarction and mortality appeared to be limited to rosiglitazone (Home *et al.*, 2005; Nissen and Wolski, 2007). These latter risks of rosiglitazone therapy have not been confirmed by other clinical studies (Rosen, 2007; Mannucci *et al.*, 2010).

In addition to the known cardiovascular side effects of rosiglitazone, the drug increased the propensity of ventricular fibrillation in pigs, an effect attributed to inhibition of the cardiac ATP-sensitive K^+ channel (Lu *et al.*, 2008). However, no direct evidence based on voltage clamp analysis is available to exclude the contribution of other ion currents. Furthermore, rosiglitazone was shown to block a wide variety of non-cardiac ion channels, including neuronal Ca^{2+} channels, epithelial Na^+ channels, ATP-sensitive K^+ channels, delayed rectifier K^+ channels and L-type Ca^{2+} channels in aortic smooth muscle cells (Knock *et al.*, 1999; Mishra and Aaronson, 1999; McKay *et al.*, 2000; Pancani *et al.*, 2009; Pavlov *et al.*, 2009). In contrast to the lack of data on cardiac cells with rosiglitazone, another thiazolidinedione derivative troglitazone was shown to effectively block L-type Ca^{2+} current (I_{Ca}) in ventricular myocytes of guinea pigs (Nakajima *et al.*, 1999; Katoh *et al.*, 2000) and rats (Arikawa *et al.*, 2002; 2004), while in rabbit ventricular cells Na^+, Ca^{2+} and K^+ currents were suppressed by the drug (Ikeda and Watanabe, 1998).

In absence of relevant voltage clamp data on the effects of rosiglitazone in mammalian cardiac preparations, we aimed to study the concentration-dependent effects of rosiglitazone on action potential morphology and the underlying ion currents in isolated canine ventricular cardiomyocytes. Canine ventricular cells were chosen because their electrophysiological properties are believed to be very similar to those of human regarding the distribution and kinetic properties of transmembrane ion currents (Szabó *et al.*, 2005; Szentandrássy *et al.*, 2005).

Methods

Isolation of single ventricular myocytes from dog heart

All animal care and experimental procedures conformed to 'Principles of laboratory animal care' (NIH publication N° 85–23, revised 1985) and were approved by the local ethical committee. Adult beagle dogs of either sex were anaesthetized with intravenous injections of 10 mg·kg^{-1} ketamine hydrochloride (Calypsol, Richter Gedeon, Budaspest, Hungary) + 1 mg·kg^{-1} xylazine hydrochloride (Sedaxylan, Eurovet Animal Health BV, Bladel, The Netherlands). The hearts were quickly removed and placed in Tyrode solution. Single myocytes were obtained by enzymatic dispersion using the segment perfusion technique (Szabó *et al.*, 2005). Briefly, a wedge-shaped section of the ventricular wall supplied by the left anterior descending coronary artery was dissected, cannulated and perfused with oxygenized Tyrode solution containing: NaCl 144, KCl 5.6, $CaCl_2$ 2.5, $MgCl_2$ 1.2, HEPES 5, and dextrose 11 mM at pH = 7.4. Perfusion was continued until all blood was washed from the coronary system and then switched to a nominally Ca^{2+}-free Joklik solution (Minimum Essential Medium Eagle, Joklik Modification, Sigma-Aldrich Co., St. Louis, MO, USA) for 5 min. This was followed by 30 min perfusion with Joklik solution supplemented with 1 mg·mL^{-1} collagenase (Type II., Worthington Biochemical Co., Lakewood, NJ, USA) and 0.2% bovine serum albumin (Fraction V., Sigma-Aldrich Co.) containing 50 μM Ca^{2+}. Portions of the left ventricular wall were cut into small pieces and the cell suspension obtained at the end of the procedure, predominantly from the mid myocardial region of the left ventricle, was washed with Joklik solution. Finally the Ca^{2+} concentration was gradually restored to 2.5 mM. The cells were stored in minimum essential medium until use.

Recording of action potentials

All electrophysiological measurements were performed at 37°C. The rod-shaped viable cells showing clear striations were sedimented in a plexiglass chamber allowing continuous superfusion with oxygenated Tyrode solution. Transmembrane potentials were recorded using 3 M KCl filled sharp glass microelectrodes having tip resistance between 20 and 40 MΩ. These electrodes were connected to the input of an Axoclamp-2B amplifier (Axon Instruments Inc., Foster City, CA, USA). The cells were paced through the recording electrode at a steady cycle length of 1 s using 1 ms wide rectangular current pulses with 120% threshold amplitude. Because the cytosol was not dialysed, time-dependent changes in action potential duration were negligible for at least 60 min under these experimental conditions (Horváth *et al.*, 2006).

Concentration-dependent effects of rosiglitazone were determined in a cumulative manner by applying increasing concentrations of the drug between 1 and 100 μM. Each concentration was superfused for 3 min and the washout usually lasted for 10 min. These incubation and washout periods were sufficient to develop steady-state drug effects and practically full reversal. As the stimulus threshold was gradually increased during the cumulative application of rosiglitazone, the amplitude of stimuli had to be increased accordingly. Action potentials were digitized at 200 kHz using Digidata 1200 A/D card (Axon Instruments Inc.) and stored for later analysis.

Conventional voltage clamp

The cells were superfused with oxygenated Tyrode solution. Suction pipettes, fabricated from borosilicate glass, had a tip resistance of 2 MΩ after filling with pipette solution containing (in mM) K-aspartate, 100; KCl, 45; $MgCl_2$, 1; HEPES, 5; EGTA, 10; K-ATP, 3, or alternatively, KCl, 110; KOH, 40; HEPES, 10; EGTA, 10; TEACl, 20; K-ATP, 3, when measuring potassium or calcium currents respectively (pH = 7.2 in both cases). Membrane currents were recorded with the Axopatch-2B amplifier using the whole cell configuration of

the patch clamp technique (Hamill *et al.*, 1981). After establishing a high (1–10 GΩ) resistance seal by gentle suction, the cell membrane beneath the tip of the electrode was disrupted by further suction or by applying 1.5 V electrical pulses for 1 ms. The series resistance was typically 4–8 MΩ before compensation (usually 50–80%). Experiments were discarded when the series resistance was high or substantially increasing during the measurement. Outputs from the clamp amplifier were digitized at 100 kHz under software control (pClamp 6.0, Axon Instruments Inc.). Ion currents were normalized to cell capacitance, determined in each cell using short hyperpolarizing pulses from –10 to –20 mV. Cell capacitance was 131 ± 5 pF in the average of 25 myocytes. The experimental protocol for each measurement is described where pertinent in the Results section. Concentration-dependent effects of rosiglitazone were determined in a cumulative manner by applying increasing concentrations of the drug between 1 and 300 μM.

Action potential voltage clamp

Using the whole cell configuration of the patch clamp technique, action potentials were recorded in current clamp mode from the myocytes superfused with Tyrode solution. The pipette solution was identical to that used for potassium current measurement under conventional voltage clamp conditions. The cells were continuously paced through the recording electrode at a steady stimulation frequency of 1 Hz so a 1–2 ms gap between the stimulus artefact and the upstroke of the action potential could occur. Ten subsequent action potentials were recorded from each cell, which were analysed online. One of these action potentials, having an APD_{90} value closest to the average of the 10 recorded action potentials, was delivered to the same cell at the identical frequency as command voltage after switching the amplifier to voltage clamp mode. The current trace obtained under these conditions is a horizontal line positioned at the zero level except for the very short segment corresponding to the action potential upstroke (Fischmeister *et al.*, 1984). Rosiglitazone was applied in a cumulative manner using concentrations of 1, 10 and 100 μM. The profile of the ion currents blocked by rosiglitazone was determined by subtracting the post-drug curve from the pre-drug curve. This procedure resulted in composite current profiles containing three distinct current peaks: an early outward peak for the transient outward K^+ current (I_{to}), an inward peak for the I_{Ca} and a late outward peak for the rapid delayed rectifier K^+ current (I_{Kr}) (Bányász *et al.*, 2007).

Statistics

Results are expressed as mean ± SEM values. Statistical significance of differences was evaluated using one-way ANOVA followed by Student's *t*-test. Differences were considered significant when $P < 0.05$. For each type of experiment, both the number of myocytes studied and the number of animals used are specified.

Materials

Rosiglitazone was freshly diluted with Tyrode solution to final concentration on the day of experiment. Rosiglitazone was purchased from Molekula Ltd (Shaftesbury, UK); all other drugs were obtained from Sigma-Aldrich Co. Drug and molecular target nomenclature follows Alexander *et al.* (2009).

Results

Effect of rosiglitazone on action potential configuration

Rosiglitazone treatment caused complex, concentration-dependent, changes in action potential morphology in canine ventricular myocytes (eight cells from four dogs), paced at a constant frequency of 1 Hz, including reduction of the amplitude of early (phase-1) repolarization, the maximum velocity of depolarization (V_{max}), and depression of the plateau potential (Figure 1A). These effects of rosiglitazone were significant at concentrations of 10 μM and higher (Figure 1B and C). Action potential duration was little affected by rosiglitazone; however, APD_{50} was significantly shortened by 30 μM, while APD_{90} was lengthened by 100 μM of rosiglitazone (Figure 1D). In spite of the reduction of V_{max}, the amplitude of action potential was not decreased by rosiglitazone. In contrast, it was significantly increased in the presence of 100 μM rosiglitazone (Figure 1E). All these effects of rosiglitazone developed rapidly (within 2–3 min) and were readily reversible after superfusion with rosiglitazone-free Tyrode solution for 10 min.

Effect of rosiglitazone on the density and kinetics of cardiac ion currents measured by conventional voltage clamp

In these experiments, performed under conventional voltage clamp conditions, cumulative concentration-dependent drug effects were monitored between 1 and 300 μM, increasing the concentration of rosiglitazone usually in steps of 0.5 log units. Kinetic properties of the channel gating were studied at concentrations, which were close to the half effective blocking concentration of rosiglitazone on the given ion current.

I_{to} was activated by depolarizations to +50 mV arising from the holding potential of –80 mV and having duration of 200 ms. Before each test pulse, a short (5 ms) depolarization to –40 mV was applied in order to inactivate the fast Na^+ current (I_{Na}), while I_{Ca} and I_{Kr} were blocked by 5 μM nifedipine and 1 μM E4031 respectively. I_{to} was suppressed by rosiglitazone in a concentration-dependent manner in the five myocytes studied (each from a different animal). This effect of rosiglitazone was statistically significant at concentrations ≥10 μM, the EC_{50} value was 25.2 ± 2.7 μM, and the Hill coefficient 1.27 ± 0.19 (Figure 2A and B). The effect of rosiglitazone developed rapidly (within 2–3 min) and was fully reversible upon washout (Figure 2C). Rosiglitazone altered the gating properties of I_{to}. The current inactivated as a sum of a faster and a slower component. The amplitude of both components was significantly decreased in the presence of 30 μM rosiglitazone. The fast time constant was not modified, while the slow time constant was doubled by rosiglitazone (Figure 2D). Activation of I_{to} required larger depolarizations in the presence of rosiglitazone and the activation threshold was shifted from –20 to +20 mV (Figure 2E), while no significant change was observed in the voltage-dependence of inactivation (Figure 2F).

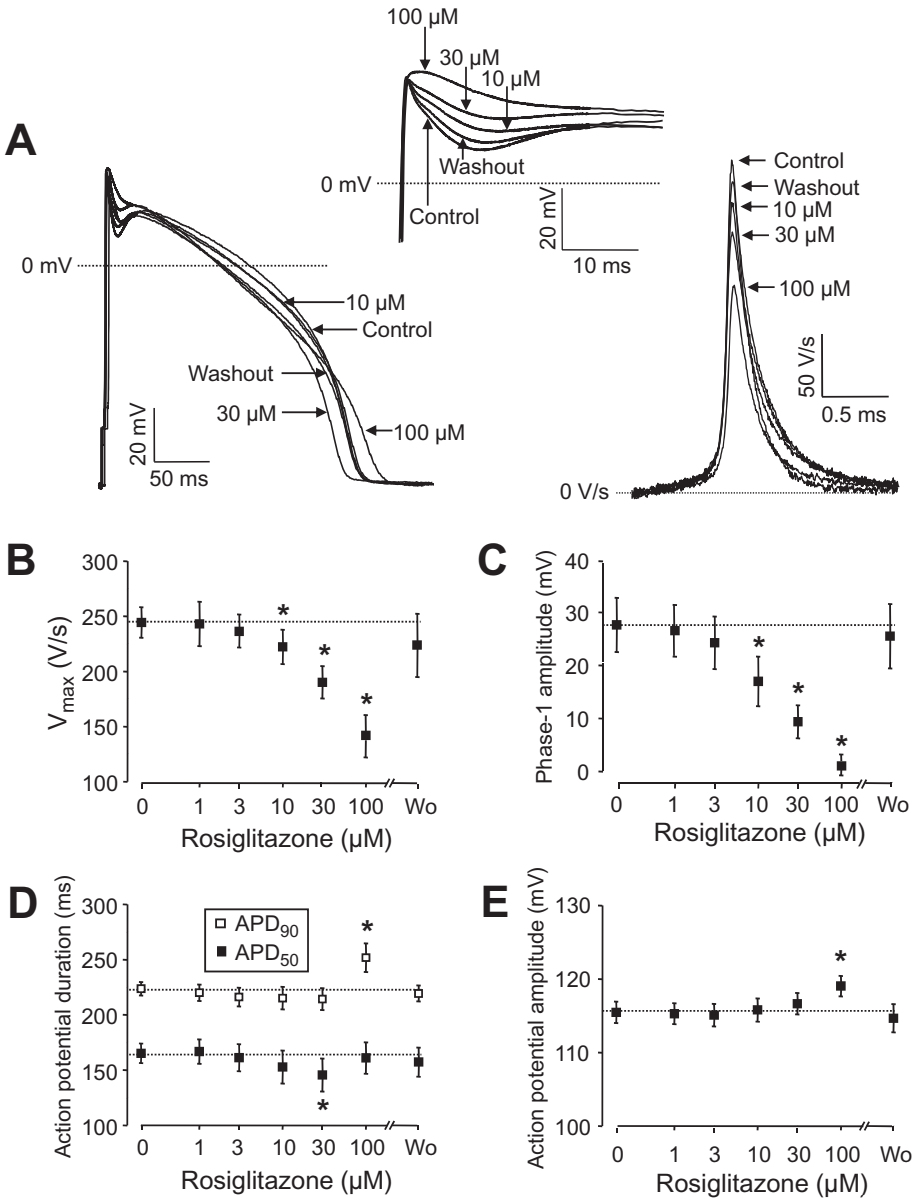

Figure 1

(A) Representative set of superimposed action potentials showing the cumulative concentration-dependent effects of rosiglitazone on action potential configuration. Early events of the action potential are enlarged in the inset, the first time derivatives of action potential upstrokes are depicted on the right. The action potentials were superimposed so as to match their upstrokes. (B–E) Cumulative concentration-dependent effects of rosiglitazone on the maximum rate of depolarization (V_{max}), amplitude of phase-1 repolarization, action potential duration measured at 50% (APD_{50}) and 90% (APD_{90}) level of repolarization, and action potential amplitude respectively. Phase-1 amplitude was determined as a difference of overshoot potential and the deepest point of the incisura. Each concentration of rosiglitazone was superfused for 3 min, the washout (Wo) lasted for 10 min. Symbols and bars represent mean ± SEM values of eight myocytes, obtained from four dogs. *$P < 0.05$, significant changes from pre-drug control values, which are also indicated by dotted lines.

I_{Kr} was activated by 1 s long depolarizing pulses to +50 mV, from the holding potential of –40 mV. I_{Kr} was assessed as tail current amplitudes recorded following repolarization to the holding potential. I_{Ca} and the slow delayed rectifier K^+ current were suppressed by 5 μM nifedipine and 1 μM HMR-1556 respectively. As shown in Figure 3A and B, the amplitudes of the I_{Kr} current tails were progressively decreased by increasing concentrations of rosiglitazone. The EC_{50} value and Hill coefficient were estimated to be 72.3 ± 9.3 μM and 0.91 ± 0.1, respectively, as the mean of five myocytes, each derived from a different animal (Figure 3B). Similarly to results observed with I_{to}, suppression of the I_{Kr} tails developed rapidly and was fully reversible (Figure 3C). Relaxation of I_{Kr} current tails (deactivation) followed biexponential kinetics. Although the time constants of both components decreased, this effect failed to reach the level of

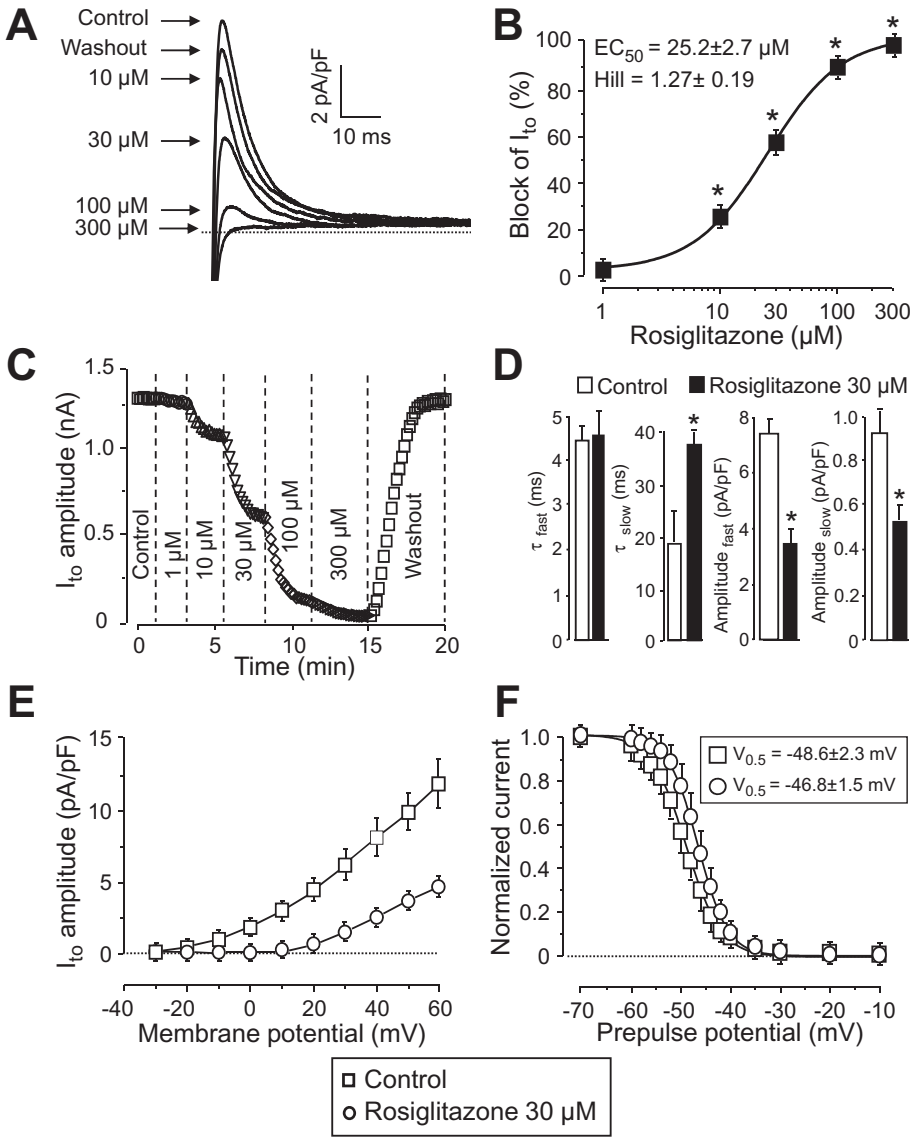

Figure 2

Effect of rosiglitazone on I_{to}. (A), (B): Cumulative concentration-dependent effects of rosiglitazone on I_{to} measured under conventional voltage clamp conditions. Representative superimposed I_{to} current traces (A**)** recorded before and after superfusion with increasing concentrations of rosiglitazone, and the dose–response curve (B) obtained for I_{to} blockade in five cells, each from a different animal, including the results of the Hill plot. (C): Time course of development and reversibility of the effect of rosiglitazone on I_{to} measured in a representative cell. (D)–(F): Effect of 30 μM rosiglitazone on kinetic properties of I_{to} studied in five myocytes, each from a different dog. (D): Time course of inactivation of I_{to}. The current decay was fitted as a sum of two (fast and slow) exponential components. (E): Current–voltage relationship obtained for I_{to}. Peak values of I_{to} were plotted against the respective test potential shown on abscissa. (F): Effect of rosiglitazone on the voltage-dependence of steady-state inactivation of I_{to}. Test depolarizations to +50 mV were preceded by a set of prepulses clamped to various voltages between −70 and +10 mV. Peak currents measured after these prepulses were normalized to the peak current measured after the −70 mV prepulse and plotted against the respective prepulse potential. Solid lines were obtained by fitting data to the two-state Boltzmann function. Symbols, columns and bars are means ± SEM. *$P < 0.05$, significant changes from control.

statistical significance ($P > 0.05$). In contrast, the amplitudes of both components were significantly reduced by 100 μM rosiglitazone. Voltage-dependence of activation of I_{Kr} was moderately shifted towards more negative potentials by 100 μM rosiglitazone: the half-activation voltage ($V_{0.5}$) of I_{Kr} was shifted from –4.8 ± 3.2 to –10.2 ± 1.3 mV (five cells, each from a different dog, $P < 0.05$). Due to this shift of activation, the block apparently increased with increasing depolarizations to more positive voltages, it was negligible at membrane potentials ≤–5 mV, while it represented close to half of control current amplitude at voltages more positive than +10 mV (Figure 3E). No change in the monoexponential time

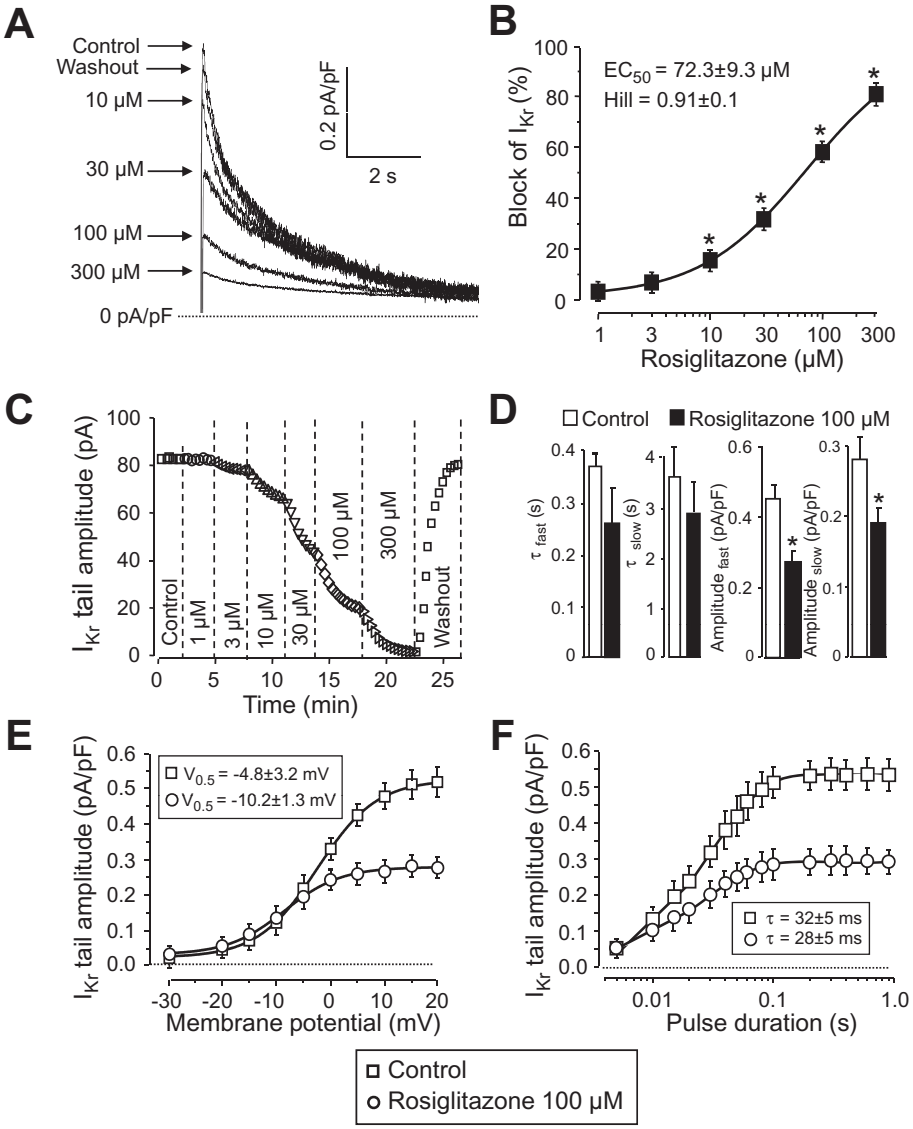

Figure 3

Effect of rosiglitazone on I_{Kr}. (A), (B): Concentration-dependent effects of rosiglitazone on I_{Kr} measured under conventional voltage clamp conditions. Representative superimposed I_{Kr} tail current traces (A) recorded before and after superfusion with increasing concentrations of rosiglitazone, and the dose–response curve (B) obtained for I_{Kr} blockade in five cells, each from a different animal, including the results of the Hill plot. (C): Time course of development and reversibility of the effect of rosiglitazone on I_{Kr} recorded from a representative cell. (D)–(F): Effect of 100 μM rosiglitazone on kinetic properties of I_{Kr} studied in five myocytes, each obtained from a different dog. (D): Time course of deactivation of I_{Kr}. Decay of tail currents was fitted as a sum of two (fast and slow) exponential components. (E): Voltage-dependence of activation of I_{Kr} was determined by varying the potential for I_{Kr} activation as indicated on the abscissa. The results were fitted to the two-state Boltzmann function denoted by solid lines. (F): Time constant of activation was determined by monoexponential fitting of data obtained using the tail envelope test (applying depolarizations to +50 mV and determining tail current amplitudes at –40 mV). Durations of these depolarizing pulses are displayed on the abscissa. Symbols, columns and bars are mean values ± SEM. *$P < 0.05$, significant changes from control.

constant of activation of I_{Kr}, determined by using the tail envelope test, was observed in the presence of 100 μM rosiglitazone (Figure 3F).

I_{Ca} was recorded at +5 mV using 400 ms long depolarizations arising from the holding potential of –40 mV. In these experiments, Tyrode solution was supplemented with 3 mM 4-aminopyridine, 1 μM E4031 and 1 μM HMR-1556 in order to block K^+ currents. Rosiglitazone blocked I_{Ca} in a concentration-dependent manner causing statistically significant block at concentrations ≥10 μM. The EC_{50} value and Hill coefficient were 82.5 ± 9.4 μM and 0.82 ± 0.08, respectively, in the six myocytes obtained from five dogs (Figure 4A and B). As indicated by Figure 4C, I_{Ca} was only partially reversed during the 10 min period of washout following rosiglitazone treatment. Rosiglitazone altered slightly the gating properties of I_{Ca} as well. This current inactivated as a sum of two exponential components and no significant changes in the time constants were observed. Although

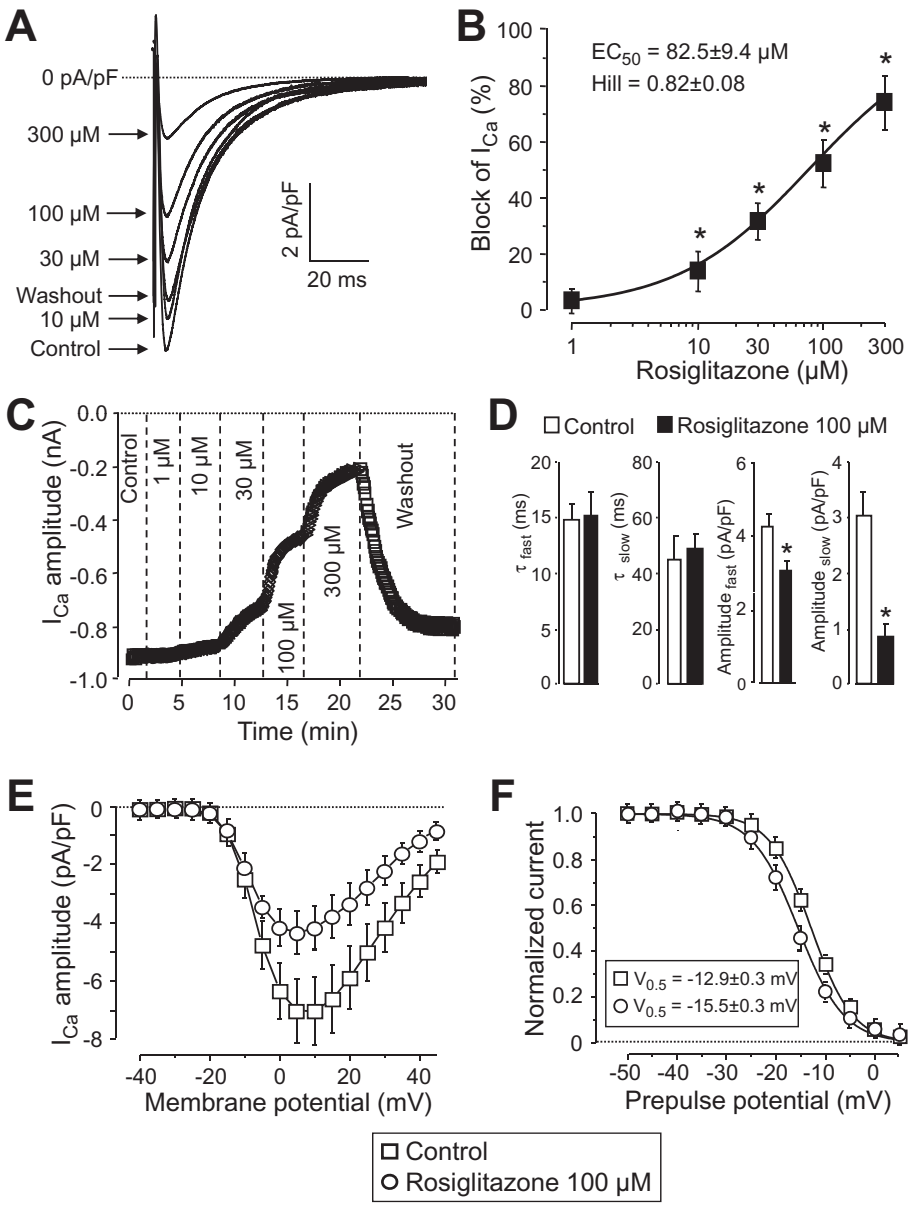

Figure 4

Effect of rosiglitazone on I_{Ca}. (A), (B): Cumulative concentration-dependent effects of rosiglitazone on I_{Ca} measured under conventional voltage clamp conditions. Representative superimposed I_{Ca} current traces (A) recorded before and after superfusion with increasing concentrations of rosiglitazone, and the dose–response curve (B) obtained for I_{Ca} blockade in six cells from five dogs, including the results of the Hill plot. (C): Time course of development and reversibility of the effect of rosiglitazone on I_{Ca} measured in a representative cell. (D)–(F): Effect of 100 µM rosiglitazone on kinetic properties of I_{Ca} studied in five myocytes, derived from five different animals. (D): Time course of inactivation of I_{Ca}. The current decay was fitted as a sum of two (fast and slow) exponential components. (E): Current–voltage relationship obtained for I_{Ca}. Amplitudes of I_{Ca} were plotted against the respective test potential shown on abscissa. (F): Effect of rosiglitazone on the voltage-dependence of steady-state inactivation of I_{Ca}. Test depolarizations to +5 mV were preceded by a set of prepulses clamped to various voltages between −50 and +5 mV. Peak currents measured after these prepulses were normalized to the peak current measured after the −50 mV prepulse and plotted against the respective prepulse potential. Solid lines were obtained by fitting data to the two-state Boltzmann function. Symbols, columns and bars are means ± SEM. *$P < 0.05$, significant changes from control.

amplitudes of both the fast and slow components were decreased by 100 µM rosiglitazone, suppression of the slow component was more pronounced. (Figure 4D). Rosiglitazone had no effect on the current–voltage relationship obtained for I_{Ca} by plotting the amplitudes of the current against the respective test potentials (Figure 4E). In contrast, steady-state inactivation of I_{Ca} was enhanced by 100 µM rosiglitazone. The half inactivation voltage ($V_{0.5}$) was significantly shifted

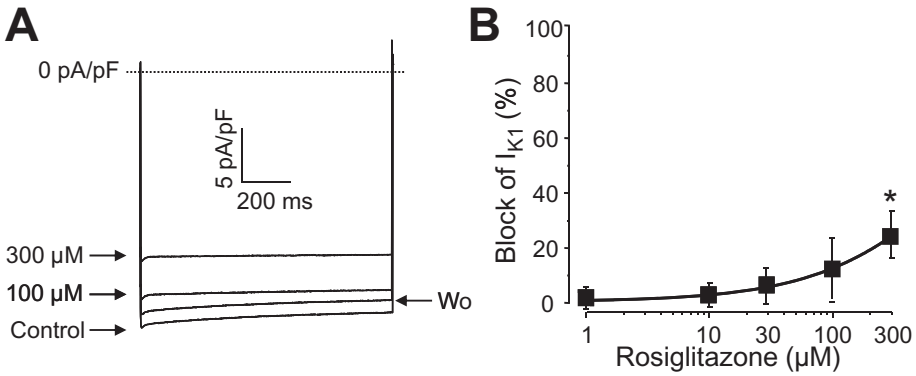

Figure 5

Cumulative concentration-dependent effects of rosiglitazone on I_{K1} measured under conventional voltage clamp conditions. Representative superimposed I_{K1} current traces (A) recorded before and after superfusion with increasing concentrations of rosiglitazone, and the dose–response curve (B) obtained for I_{K1} blockade in four cells, each from a different dog. Symbols and bars are means ± SEM. *$P < 0.05$, significant changes from control.

towards more negative potentials (from –12.9 ± 0.3 mV to –15.5 ± 0.3 mV, $P < 0.05$, five cells, each from a different animal, Figure 4F).

The inward rectifier K^+ current (I_{K1}) was studied by applying hyperpolarizations to –135 mV from the holding potential of –40 mV. The steady-state current was determined 400 ms after the beginning of the pulse. As it is shown in Figure 5, I_{K1} was not significantly modified by rosiglitazone up to the concentration of 100 μM in the four cells challenged, each obtained from a different dog. Above this concentration (at 300 μM) a small but fully reversible suppression of I_{K1} was observed.

Effect of rosiglitazone on ion currents under action potential clamp conditions

The profile of an ion current may be markedly different when comparing under conventional voltage clamp and action potential clamp conditions. An advantage of the action potential clamp technique is that the effect of any drug on the net membrane current can be recorded allowing thus to monitor drug effects simultaneously on more than one ion current. Furthermore, this technique enables us to record true current profiles flowing during an actual cardiac action potential. Of course, in the case of a drug acting on more than one ion current, such as rosiglitazone, a series of peaks can be detected on the current trace, each of them corresponding to the fingerprint of an individual ion current. Accordingly, the early outward current peak, shown in Figure 6, arises when I_{to} is suppressed, while the inward deflection indicates a blockade of I_{Ca}. The late outward current peak, coincident with terminal repolarization of the canine action potential, is a mixture of I_{Kr} plus I_{K1}. In our case, however, it is likely caused by pure I_{Kr} blockade, because – as we have previously shown – I_{K1} was not affected by 100 μM rosiglitazone. As demonstrated in Figure 6, rosiglitazone suppressed I_{to}, I_{Kr} and I_{Ca} under action potential voltage clamp conditions in a concentration-dependent and largely reversible manner – in line with results of conventional voltage clamp experiments. The amplitudes of the three current peaks (early outward, inward and late outward) are presented in Figure 7 as the mean of five myocytes, each obtained from a different dog.

Discussion

Effects of rosiglitazone on action potential morphology are in line with effects on the underlying ion currents

Effects of rosiglitazone on native cardiac ion currents were first analysed in this study. The results revealed that rosiglitazone suppressed several ion currents, including I_{Na}, I_{to}, I_{Kr} and I_{Ca}, in a concentration-dependent manner with the concomitant alterations in the configuration of the action potential. These changes can be associated with suppression of various ion currents with concomitant changes in channel gating. For instance, the rosiglitazone-induced decrease in phase-1 repolarization may be due to reduction of I_{to}. Similarly, the depression of the plateau, observed in the presence of rosiglitazone, may be a consequence of inhibition of Ca^{2+} and Na^+ currents. Concentration-dependent blockade of I_{to} and I_{Ca} have been demonstrated by our present voltage clamp experiments, while the observed suppression of V_{max} is believed to be a good indicator of I_{Na} blockade (Strichartz and Cohen, 1978).

In spite of the multiple actions of rosiglitazone on cardiac ion channels, action potential duration was little affected by rosiglitazone, except for the moderate reduction of APD_{50} at 30 μM and lengthening of APD_{90} at 100 μM concentration. This apparently paradoxical behaviour may be related to differences in blocking potencies on the various ion currents. On the other hand, the lack of marked effects of rosiglitazone on action potential duration suggests that inhibition of inward (window I_{Na} and I_{Ca}) and outward (I_{Kr} and I_{to}) currents are relatively well compensated. This suggestion is strongly supported by the action potential voltage clamp records shown in Figure 6. Also, suppression of V_{max} is usually accompanied with reduction of action potential amplitude. This effect was not observed with rosiglitazone – in contrast –

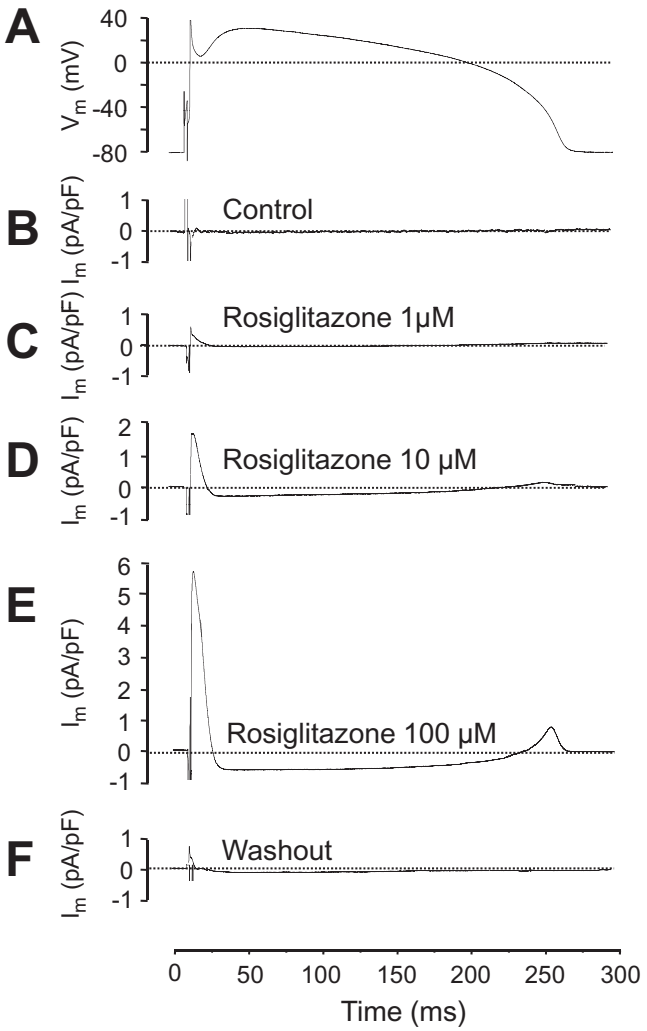

Figure 6

Effects of 1, 10 and 100 μM rosiglitazone on ion currents under action potential voltage clamp conditions. Representative records of a command signal (A), and the underlying current traces obtained before (B), in the presence of (C)–(E), and after washout of rosiglitazone (F). Because ion currents were obtained from the same cell that provided the command action potential, the pre-drug current record was a horizontal line at the zero level. The post-drug difference currents have been inverted in order to present the currents with their conventional polarity. Dotted lines indicate zero current level for each trace except for (A), where it represents zero voltage.

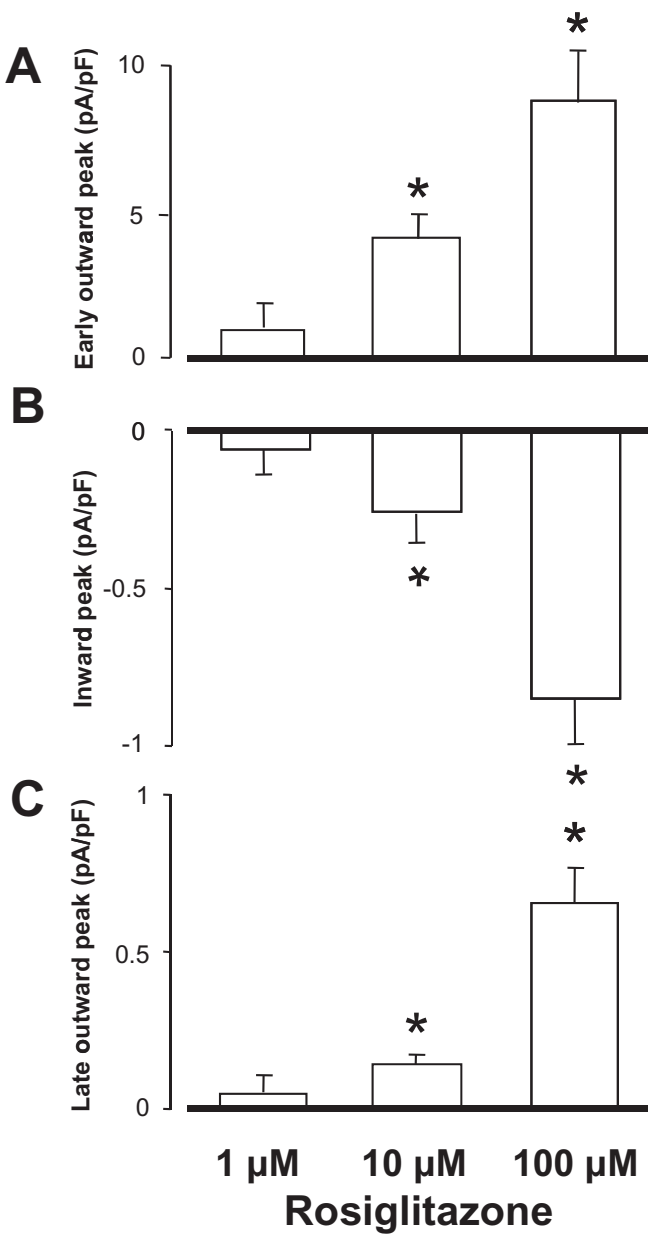

Figure 7

Effects of 1, 10 and 100 μM rosiglitazone on the early outward current peak, indicator of I_{to} (A), the inward current peak, indicator of I_{Ca} (B), and the late outward current peak, indicator predominantly of I_{Kr} (C), obtained under action potential voltage clamp conditions in five myocytes, each from a different animal. Columns and bars are means ± SEM. *$P < 0.05$, significant changes from control.

action potential amplitude was significantly increased by the highest rosiglitazone concentration applied (100 μM). This effect is likely to be due to the simultaneous blockade of I_{Na} and I_{to}, with the former effect tending to decrease, and the latter tending to increase, the amplitude of action potentials. Finally, the lack of depolarization is compatible with the inability of rosiglitazone to alter I_{K1} at concentrations up to 100 μM.

Comparison with troglitazone

Our present results allow some comparison between the cellular cardiac electrophysiological effects of rosiglitazone and troglitazone. Troglitazone blocked I_{Ca} with IC_{50} values close to 10 μM in rat (Arikawa *et al.*, 2002; 2004), rabbit (Ikeda and Watanabe, 1998) and guinea pig (Nakajima *et al.*, 1999) myocytes. This value is significantly smaller than the IC_{50} of 92 μM obtained with rosiglitazone in canine ventricular cells (present study). The inhibitory effect of troglitazone on I_{Na} is also much stronger than that of rosiglitazone. In contrast to our results, where 100 μM rosiglitazone caused less than 50% reduction of V_{max}, 1 μM of troglitazone induced 50% V_{max}

blockade, while 10 μM of the compound fully eliminated action potentials in rabbit ventricular myocytes (Ikeda and Watanabe, 1998). Thus the difference between the inhibiting potency of rosiglitazone and troglitazone seems to be at least one order of magnitude. In summary, as rosiglitazone is a weaker inhibitor of cardiac ion channels than the other thiazolidinedione derivative troglitazone, less cardiac side effects would be anticipated with rosiglitazone than with troglitazone.

Clinical implications

The lowest concentration of rosiglitazone that caused statistically significant changes in our study was much higher than the peak plasma levels obtained in patients. Peak plasma concentration of 0.8 $\mu g \cdot mL^{-1}$ (corresponding to 2 μM) is typical in patients after receiving a single dose of 8 mg rosiglitazone (Park *et al.*, 2004; Wittayalertpanya *et al.*, 2010). Therefore, it is not likely that rosiglitazone, in normal doses, would alter cardiac electrogenesis in healthy individuals. In line with this, no case of sudden death has been reported in association with rosiglitazone therapy. But what might happen with a rosiglitazone overdose? Under such non-normal conditions, rosiglitazone concentrations in the plasma are likely to reach a much higher level, probably several tens of micromoles, where a variety of cardiac ion channels could be suppressed thus favouring the development of cardiac arrhythmias. This may be especially dangerous in patients with multiple cardiovascular risk factors, like elderly diabetic patients with ischemic heart disease. Indeed, rosiglitazone has been shown to increase the propensity for ventricular fibrillation in ischemic pigs (Lu *et al.*, 2008). Thus the pro-arrhythmic action of rosiglitazone may be combined with, and contribute to, the development of other unfavourable cardiac side effects observed in an at-risk group of diabetic patients. This is in line with the consensus statement of the American and European Diabetes Associations, advising clinicians against using rosiglitazone in patients with type 2 diabetes mellitus (Krentz, 2009; Kaul *et al.*, 2010).

Limitations of the study

The present results with rosiglitazone were obtained in healthy canine hearts, while rosiglitazone is usually given to diabetic patients. Diabetes is known to induce marked remodelling in the set of cardiac ion currents in all mammalian species studied, including dogs (Lengyel *et al.*, 2007), rabbits (Lengyel *et al.*, 2008) and rats (Magyar *et al.*, 1992). In addition, differences in the effects of both rosiglitazone and troglitazone were observed when compared between healthy and diabetic rats (Arikawa *et al.*, 2002; Kavak *et al.*, 2008). Our data therefore should be extrapolated to diabetic patients with caution.

Acknowledgements

Financial support for the studies was provided by grants from the Hungarian Scientific Research Fund (OTKA-K68457, OTKA-K73160, CNK-77855). Further support was obtained from the Hungarian Government (TÁMOP-4.2.1/B-09/1/KONV-2010–007), and the Medical and Health Science Center of University of Debrecen (MEC-14/2008).

Conflicts of interest

None.

References

Alexander SPH, Mathie A, Peters, JA (2009). Guide to Receptors and Channels (GRAC), 4th edition. Br J Pharmacol 158 (Suppl. 1): S1–S180.

Arikawa M, Takahashi N, Kira T, Hara M, Saikawa T, Sakata T (2002). Enhanced inhibition of L-type calcium currents by troglitazone in streptozotocin-induced diabetic rat cardiac ventricular myocytes. Br J Pharmacol 136: 803–810.

Arikawa M, Takahashi N, Kira T, Hara M, Yoshimatsu H, Saikawa T (2004). Attenuated inhibition of L-type calcium currents by troglitazone in fructose-fed rat cardiac ventricular myocytes. J Cardiovasc Pharmacol 44: 109–116.

Bányász T, Magyar J, Szentandrássy N, Horváth B, Birinyi P, Szentmiklósi J *et al.* (2007). Action potential clamp fingerprints of K^+ currents in canine cardiomyocytes: their role in ventricular repolarization. Acta Physiol (Scand) 190: 189–198.

Berger J, Bailey P, Biswas C, Cullinan CA, Doebber TW, Hayes NS *et al.* (1996). Thiazolidinediones produce a conformational change in peroxisomal proliferator-activated receptor-gamma: binding and activation correlate with antidiabetic actions in db/db mice. Endocrinology 137: 4189–41950.

Cuzzocrea S, Pisano B, Dugo L, Patel NS, Paola RD, Genovese T *et al.* (2003). Rosiglitazone and 15-deoxy-$^{\Delta 12,14}$- prostaglandin J_2 ligands of the peroxisome proliferator-actvated receptor-γ (PPAR-γ) reduce ischemia/reperfusion injury of the gut. Br J Pharmacol 140: 366–376.

Doshi LS, Brahma MK, Bahirat UA, Dixit AV, Nemmani KV (2010). Discovery and development of selective PPARgamma modulators as safe and effective antidiabetic agents. Expert Opin Investig Drugs 19: 489–512.

DREAM Trial Investigators: Dagenais GR, Gerstein HC, Holman R, Budaj A, Escalante A, Hedner T *et al.* (2008). Effects of ramipril and rosiglitazone on cardiovascular and renal outcomes in people with impaired glucose tolerance or impaired fasting glucose: results of the Diabetes REduction Assessment with ramipril and rosiglitazone Medication (DREAM) trial. Diabetes Care 31: 1007–1014.

Fischmeister R, DeFelice LJ, Ayer RK, Levi R, DeHaan RL (1984). Channel currents during spontaneous action potentials in embryonic chick heart sells. The action potential patch clamp. Biophys J 46: 267–271.

Gerstein HC, Yusuf S, Bosch J, Pogue J, Sheridan P, Dinccag N *et al.* (2006). Effect of rosiglitazone on he frequency of diabetes in patients with impaired glucose tolerance or impaired fasting glucose: a randomised controlled trial DREAM (Diabetes Reduction Assessment with ramipril and rosiglitazone Medication). Lancet 368: 1096–1105.

Hamill OP, Marty A, Neher E, Sakmann B, Sigworth FJ (1981). Improved patch-clamp techniques for high-resolution current recording from cells and cell-free membrane patches. Pflugers Arch 391: 85–100.

Home PD, Pocock SJ, Beck-Nielsen H, Gomis R, Hanefeld M, Dargie H *et al.* (2005). Rosiglitazone evaluated for cardiac outcomes and regulation of glycaemia in diabetes (RECORD): study design and protocol. Diabetologia 48: 1726–1735.

Horváth B, Magyar J, Szentandrássy N, Birinyi P, Nánási PP, Bányász T (2006). Contribution of I_{Ks} to ventricular repolarization in canine myocytes. Pflugers Arch 452: 698–706.

Ikeda S, Watanabe T (1998). Effects of troglitazone and pioglitazone on the action potentials and membrane currents of rabbit ventricular myocytes. Eur J Pharmacol 357: 243–250.

Katoh Y, Hashimoto S, Kimura J, Watanabe T (2000). Inhibitory action of troglitazone, an insulin-sensitising agent, on the calcium current in cardiac ventricular cells of guinea pig. Jpn J Pharmacol 82: 102–109.

Kaul S, Bolger AF, Herrington D, Guiliano RP, Eckel RH (2010). Thiazolidinedione drugs and cardiovascular risks. A science advisory from the American Heart Association and American College of Cardiology Foundation. Circulation 21: 1868–1877.

Kavak S, Emre M, Tetiker T, Kavak T, Kolcu Z, Günay I (2008). Effects of rosiglitazone on altered electrical left ventricular papillart muscle activities of diabetic rat. Naunyn-Schmiedberg's Arch Pharmacol 376: 415–421.

Khandoudi N, Delerive P, Berrebi-Bertrand I, Buckingham RE, Staels B, Bril A (2002). Rosiglitazone, a peroxisome proliferator-activated receptor-γ, inhibits the Jun NH_2-terminal kinase activating protein 1 pathway and protects the heart from inschemic/reperfusion injury. Diabetes 51: 1507–1514.

Knock GA, Mishra SK, Aaronson PI (1999). Differential effects of insulin-sensitizers troglitazone and rosiglitazone on ion currents in rat vascular smooth muscle. Eur J Pharmacol 368: 103–109.

Krentz A (2009). Thiazolidinediones: effects of the development and progression of type 2 diabetes and associated vascular complications. Diabetes Metab Res Rev 25: 112–126.

Lengyel C, Virág L, Bíró T, Jost N, Pacher P, Magyar J *et al.* (2007). Diabetes mellitus attenuates the repolarization reserve in mammalian heart. Cardiovasc Res 73: 512–520.

Lengyel C, Virág L, Pacher P, Kocsis E, Nánási PP, Tóth M *et al.* (2008). Analysis of the electrophysiological effects of the alloxan induced diabetes mellitus in rabbit heart. Acta Physiol Scand 192: 359–368.

Lu L, Reiter MJ, Xu Y, Chicco A, Greyson CR, Schwartz GG (2008). Thiazolidinedione drugs block cardiac K_{ATP} channels and may increase propensity for ischemic ventricular fibrillation in pigs. Diabetologia 51: 675–685.

McGuire DK, Inzucchi SE (2008). Drugs for the treatment of diabetes mellitus. Part I: Thiazolidinediones and their evolving cardiovascular implications. Circulation 117: 440–449.

McKay NG, Kinsella JM, Campbell CM, Ashford ML (2000). Sensitivity of Kir6.2-SUR1 currents, in the absence and presence of sodium azide, to the K_{ATP} channel inhubitors, ciclazindole and englitazone. Br J Pharmacol 130: 857–866.

Magyar J, Rusznák Z, Szentesi P, Szucs G, Kovács L (1992). Action potentials and potassium currents in rat ventricular muscle during experimental diabetes. J Mol Cell Cardiol 24: 841–853.

Mannucci E, Monami M, Di Bari M, Lamanna C, Gori F, Gensini GF *et al.* (2010). Cardiac safety profile of rosiglitazone. A comprehensive meta-analysis of randomised clinical trials. Int J Cardiol 143: 135–140.

Mishra SK, Aaronson PI (1999). Differential block by troglitazone and rosiglitazone of glibenclamide-sensitive K^+ current in rat aorta myocytes. Eur J Pharmacol 368: 121–125.

Nakajima T, Iwasawa K, Oonuma H, Imuta H, Hazama H, Asano M *et al.* (1999). Troglitazone inhibits voltage-dependent calcium currents in guinea pig cardiac myocytes. Circulation 99: 2942–2950.

Nissen SE, Wolski K (2007). Effect of rosiglitazone on the risk of myocardial infarction and death from cardiovascular causes. N Engl J Med 357: 2461–2471.

Pancani T, Phelps JT, Searcy JL, Kilgore MW, Chen KC, Porter NM *et al.* (2009). Distinct modulation of voltage-gated and ligand-gated Ca^{2+} currents by PPAR-gamma agonists in cultured hipocampal neurons. J Neurochem 109: 1800–1811.

Park J-Y, Kim K-A, Shin J-G, Lee KY (2004). Effect of ketoconazole on the pharmacokinetics of rosiglitazone in healthy subjects. Br J Clin Pharmacol 58: 397–402.

Pavlov TS, Levchenko VL, Karpushev AV, Vandewalle A, Staruschenko A (2009). Peroxisome proliferators-activated receptor gamma antagonists decrease Na^+ transport via the epithelial Na^+ channel. Mol Pharmacol 76: 1333–1340.

Quinn CE, Hamilton PK, Lockhart CJ, McVeigh GE (2008). Thiazolidinediones: effects on insulin resistance and the cardiovascular system. Br J Pharmacol 153: 636–645.

Rosen JC (2007). The rosiglitazone story: lessons from an FDA Advisory Committee meeting. N Engl J Med 357: 844–846.

Strichartz G, Cohen I (1978). V_{max} as a measure of G_{Na} in nerve and cardiac membranes. Biophys J 23: 153–156.

Szabó G, Szentandrássy N, Bíró T, Tóth IB, Czifra G, Magyar J *et al.* (2005). Asymmetrical distribution of ion channels in canine and human left ventricular wall: epicardium versus midmyocardium. Pflugers Arch 450: 307–316.

Szentandrássy N, Bányász T, Bíró T, Szabó G, Tóth IB, Magyar J *et al.* (2005). Apico-basal inhomogeneity in distribution of ion channels in canine and human ventricular myocardium. Cardiovasc Res 65: 851–860.

Welters HJ, McBain SC, Tadayyon M, Scarpello JH, Smith SA, Morgan NG (2004). Expression and functional activity of PPAR-γ in pancreatic beta cells. Br J Pharmacol 142: 1162–1170.

Wittayalertpanya S, Chompootaveep S, Thaworn N, Khemsri W, Intanil N (2010). Oharmacokinetic and bioequivalence study of an oral 8 mg dose of rosiglitazone tablets in Thai healthy volunteers. J Med Assoc Thai 93: 722–728.